Conformations and Dynamics of the Essential Cysteinyl-Cysteine Ring Derived from the Acetylcholine Receptor[†,‡]

Daina Z. Avizonis, Shauna Farr-Jones, Phyllis Anne Kosen, and Vladimir J. Basus*

Contribution from the Department of Pharmaceutical Chemistry, University of California—San Francisco, San Francisco, California 94143-0446

Received June 14, 1996[⊗]

Abstract: The nicotinic acetylcholine receptor exists in different conformational states which are modulated by the binding of acetylcholine and are responsible for the regulation of ion transport across the cell membrane. How structural transitions are induced from the acetylcholine binding site to the ion channel is still a mystery. One hypothesis suggests that an invariant cysteinyl-cysteine ring in the N-terminal region of the α-subunit of all acetylcholine receptors may act as a molecular switch contributing to allosteric rearrangements. Since the cysteinyl-cysteine ring is a highly constrained structural element, we synthesized a peptide containing this ring, corresponding to amino acids 191 to 195 of the α-subunit of the receptor. This peptide (TCCPD) has four conformations, as characterized by both natural abundance ^{13}C and proton NMR spectroscopy in aqueous solution. Both *cis* and *trans* conformations for the amide bond between the two cysteines were observed. Exchange rates between the two *cis* conformations and between *cis* and *trans* conformations were measured by indirectly detected ^{13}C NMR. The $\Delta G^{\ddagger}$ at 20 °C was 15 and 21 kcal/mol, respectively. These barriers were within 1 kcal/mol of energy barriers calculated by molecular mechanics. Our results show the cysteine-cysteinyl ring can adopt multiple conformations and exchange between them. The eight-membered cysteinyl-cysteine may play in important role in allosteric rearrangements of the acetylcholine receptor and other proteins where this structural element is found.

Introduction

The nicotinic-acetylcholine receptor (AChR) is a transmembrane glycoprotein of five subunits ($\alpha_2\beta\gamma\delta$), located at neuromuscular junctions of muscle cells. When an action potential is sent down the axon as a signal for muscle contraction, the neurotransmitter acetylcholine (ACh) is released into the synapse. Binding of acetylcholine to each α-subunit causes allosteric transitions to occur, opening a channel in the AChR, and cations (mostly sodium and some potassium) flow into the cells. When depolarization has reached a threshold level, muscle contraction occurs.[1,2] The AChR exists in four different states.[3] In the resting state, the channel is closed with no ligand bound. In the active state, ACh is bound to the receptor; the channel is open, and small cations pass. In the fast desensitized state or intermediate state, ACh remains bound, but the cation flow decreases 250 times compared to the active state.[4] In the slow desensitized state, no ion flux across the membrane is detectable, and the binding of ACh is 10^4 times stronger than that of the active state. It has been shown that the AChR receptor converts from the resting state to the slow desensitized state upon binding agonist or antagonist.[5−7] Changes in intrinsic and extrinsic fluorescence,[8,9] circular dichroism,[10] fourier transform infrared difference spectra,[11] plus other experimental evidence[12] indicate that the resting state is conformationally distinct from the slow desensitized state of AChR after incubation with ACh, agonist or antagonist. Spontaneous opening and desensitization of the AChR also occurs in the absence of ligand.[13−15]

The neurotransmitter binds to AChR far (approximately 30 Å) from the site of channel opening.[16,17] To date, there are no sufficiently resolved structures of AChR to explain how binding of ACh causes such large structural changes in the receptor. One hypothesis suggests the existence of a molecular switch at the ACh binding site.[18] The ACh binding site and that of other ligands, including α-bungarotoxin, is located at the extracellular N-terminal portion of the α-subunit. Unwin *et al.* (1993) proposed that three loops of the α-subunit are involved in binding agonist and antagonist.[17] One of these loops, residues 185−210 (*Torpedo californica* numbering), contains a rare

[†] Key words: molecular switch, nuclear magnetic resonance, heteronuclear exchange spectroscopy.

[‡] Abbreviations: NMR, nuclear magnetic resonance; AChR, acetylcholine receptor; ACh, acetylcholine; acm, acetamidomethyl; Fmoc, 9-fluorenylmethoxycarbonyl; t-Boc, *tert*-butoxycarbonyl; NOE, nuclear Overhauser effect; NOESY, nuclear Overhauser effect spectroscopy; ROESY, rotating frame spectroscopy; HSQC, heteronuclear single quantum correlated spectroscopy; standard one-letter amino-acid abbreviations are used.

[⊗] Abstract published in *Advance ACS Abstracts,* December 1, 1996.

(1) Devillers-Theiry, A.; Galzi, J.; Eisele, J. L.; Bertrand, S.; Bertrand, D.; Changeux, J. P. *J. Membrane Biol.* **1993**, *136*, 97.
(2) Ochoa, E. L. M.; Chattopadhyay, A.; McNamee, M. G. *Cellular and Molecular Neurobiology* **1989**, *2*, 141.
(3) Stroud, R. M.; McCarthy, M. P.; Shuster, M. *Biochemistry* **1990**, *29*, 11009.
(4) Walker, J. W.; Takeyasu, T.; McNamee, M. G. *Biochemistry* **1982**, *21*, 5384.
(5) Heidmann, T.; Changeux, J.-P. *Eur. J. Biochem.* **1979**, *94*, 255.
(6) Heidmann, T.; Changeux, J.-P. *Biochem. Biophys. Res. Commun.* **1980**, *97*, 889.
(7) Boyd, N.; Cohen, J. B. *Biochemistry* **1980**, *19*, 5344.
(8) Kaneda, N.; Tanaka, F.; Kohno, M.; Hayashi, K.; Yagi, K. *Arch. Biochem. Biophys.* **1982**, *281*, 376.
(9) Dunn, S. M. J.; Raftery, M. A. *Biochemistry* **1982**, *21*, 6264.
(10) Mielke, D. L.; Kaldany, R. R.; Karlin, A.; Wallas, B. A. *Biophys. J.* **1984**, *45*, 205a.
(11) Baeziger, J. E.; Miller, K. W.; Rothschild, J. K. *Biochemistry* **1993**, *32*, 5448.
(12) Heidman, T.; Changeux, J.-P. *Eur. J. Biochem.* **1979**, *94*, 281.
(13) Jackson, M. B. *Proc. Natl. Acad. Sci. U.S.A.* **1984**, *81*, 3901−4.
(14) Jackson, M. B. *Biophys. J.* **1986**, *49*, 663−71.
(15) Jackson, M. B. *Trends Biochem. Sci.* **1994**, *19*, 396−99.
(16) Herz, J. M.; Johnson, D. A.; Taylor, P. *J. Biol. Chem.* **1989**, *264*, 12439.
(17) Unwin, N. *J. Mol. Biol.* **1993**, *229*, 1101−1124.

S0002-7863(96)02005-7 CCC: $12.00

structural element of two sequential cysteines (192 and 193) that form a disulfide bond.[18−20] Reduction of this bridge significantly decreases the binding affinity of ACh.[21] Furthermore, mutation of either C192 or C193 (or both) to serines results in complete loss of ACh binding and a permanently closed channel.[22] The importance of cysteines 192 and 193 is further exemplified by their sequence conservation in all characterized acetylcholine receptors.[23]

Since 1969, it has been assumed that a strained eight-membered cysteinyl-cysteine ring must have a *cis* peptide bond based on predictions from theoretical calculations.[24] *Cis* peptide bonds have been commonly observed in proline containing peptides or proteins. *Cis* peptide bonds in proline may account for 10−30% of the total *cis*/*trans* population.[25] Certain cyclic peptides lacking proline also contain *cis* peptide bonds.[26] In the cysteinyl-cysteine dipeptide a *cis* amide bond with a right-handed helical disulfide bond was found by X-ray crystallography.[27] Two *cis* amide bond conformations were observed in $CDCl_3$ and an additional conformation (probably *trans*) in DMSO by NMR[28] for the dipeptide with a t-Boc substitution at the nitrogen of the first cysteine and esterification to a t-butyl ester of the carboxy-terminus. In contrast, the cyclic peptide, malformin (sequence: cyclo-D-cys-D-cys-L-val-D-leu-D-leu), the cysteinyl-cysteine ring was predicted by molecular mechanics calculations to exist in the *trans* amide bond conformation,[29,30] while for the peptide, LRRCCLG, the sequential cysteines have both *cis* and *trans* amide bonds.[31]

Since little is known about the structure-function relationship of the cysteinyl-cysteine ring in the acetylcholine receptor and since it is a conformationally restrained structural element, it is interesting to study the cysteinyl-cysteine ring as an independent structural element. The first peptide fragment we studied, consisting of amino acids 180−196 of the α-subunit, has at least three conformations in aqueous solution;[32] its NMR spectrum could not be completely assigned when bound to α-bungarotoxin[33] due to conformational heterogeneity and its limited solubility inhibited additional NMR studies. These findings motivated us to study a highly soluble pentapeptide, TCCPD, corresponding to α-subunit amino acids 191−195. Here, we show that this pentapeptide exits in multiple conformations with populations of both *cis* and *trans* amide bonds between cysteines 192 and 193. We also measured the exchange rates between the two *cis*-cysteinyl-cysteine conformations and between the *cis* and *trans* cysteinyl-cysteine conformations. Although the results do not prove that the ring acts as a molecular switch, the energetics of interconversion can account for a large portion of the energy required for the intact receptor to change conformations. It has been suggested that conformational changes in the cysteinyl-cysteine ring may be the initial process in the overall conformational changes of the receptor.[18] The results presented here support this intriguing hypothesis.

Results

Theoretical Molecular Modeling/Predictions. We used molecular mechanics calculations to predict the lowest energy conformations and to estimate energy barriers to interconversion between them. In order to simplify the theoretical molecular modeling and focus attention on the eight-membered ring formed by the sequential cysteines, the calculations were performed on a cysteinyl-cysteine dipeptide with the amide group of the first cysteine, and the carboxyl of the second cysteine replaced with methyl groups. The methyl groups simulate the bulkiness of the preceding and following residues, while reducing the number of conformations possible due to conformational flexibility in the remainder of the pentapeptide. Rigorous studies of the eight-membered ring hydrocarbon cyclooctane[34] and eight-membered rings with substitution of other atoms or groups of atoms for the ring carbon atoms have been carried out.[35] Thus, we were able to systematically search for energy minima, starting from each of the classical conformations of eight-membered rings and minimizing each structure thus created. Ten structures were obtained that were true minima with energies within 13 kcal/mol of the lowest energy conformation (Figure 1). Two of those contained a *cis* peptide linkage between the two cysteines, and, in the remainder, this peptide bond was found in the *trans* conformation. These different conformations interconvert via one or two bond rotations as shown in Figure 1. Two groups of structures are defined, one where the disulfide bond has positive helicity and the other with negative helicity.

The lowest energy form was the boat-chair form with negative disulfide helicity (*cis*-boat-chair−).[36] Torsional driving of the disulfide bond resulted in a barrier of 14.4 kcal/mol for changing the sign of the disulfide helicity, which converts the *cis*-boat-chair− to the *cis*-boat-chair+ conformation. All possible paths were investigated converting each of the two *cis* conformations to every *trans* conformation. The lowest path had a barrier of 19.9 kcal/mol relative to the *cis*-boat-chair−.

The lowest energy conformations with *trans*-cysteinyl-cysteine peptide linkages were the chair-chair− and the twist-chair+ conformations. All other conformations were at least 4.7 kcal/mol higher in energy than the lowest *trans* conformation, so they will not be significantly populated at room temperature. Nevertheless, all paths involving these higher energy intermediates in the interconversion between the two lowest energy *trans* conformations were investigated in order to find the lowest energy path from the twist-chair+ to the chair-chair− conformation. The lowest path found goes through the *trans*-boat-chair β1−conformation and has a barrier of 13.5 kcal/mol relative to the lowest *cis* conformation and 13.0 kcal/mol relative to the lowest energy *trans* conformation, so that, at 25°C,

(18) Kao, P. N.; Karlin, A. *J. Biol. Chem.* **1986**, *261*, 8085−8088.
(19) Kao, P. N.; Dwork, A. J.; Kaldany, R. R. J.; Silver, M. L.; Widemann, J.; Stein, S.; Karlin, A. *J. Biol. Chem.* **1984**, *259*, 11662−11665.
(20) Mosckovitz, R.; Gershoni, J. M. *J. Biol. Chem.* **1988**, *263*, 1017−1022.
(21) Walker, J. W.; Lukas, R. J.; McNamee, M. G. *Biochemistry* **1981**, *20*, 2191−2193.
(22) Mishina, M.; Tobimatsu, T.; Imoto, I.; Tanaka, K.; Fujita, Y.; Fukuda, K.; Kurasaki, M.; Takahashi, H.; Morimoto, Y.; Hirose, T.; Inayama, S.; Takahashi, T.; Kuno, M.; Numa, S. *Nature* **1985**, *313*, 364−369.
(23) McLane, K. E.; Wu, X.; Conti-Tronconi, B. M. *Biochemistry* **1991**, *30*, 10730−10738, and references therein.
(24) Chandrasekaran, R.; Balasubramanian, R. *Biochim. Biophys. Acta* **1969**, *188*, 1−9.
(25) London, R. E.; Matwiyoff, N. A.; Stewart, J. M.; Cann, J. R. *Biochemistry* **1978**, *17*, 2277−83.
(26) Mierke, D. F.; Yamazaki, T.; Said-Nejad, O. E.; Felder, E. R.; Goodman, M. *J. Am. Chem. Soc.* **1989**, *111*, 6847−6849.
(27) Capasso, S.; Mattia, C. A.; Mazzarella, L.; Puliti, R. *Acta Crystallogr. Sect B* **1977**, *33*, 2080−2083.
(28) Horne, A.; North, M.; Parkinson, J. A.; Sadler, I. H. *Tetrahedron* **1993**, *49*, 5891−5904.
(29) Mitra, A. K.; Chandrasekaran, R. *Biopolymers* **1984**, *23*, 2513−24.
(30) Tonelli, A. E. *Biopolymers* **1978**, *17*, 1175−1179.
(31) Sukumaran, D. K.; Prorok, M.; Lawrence, D. S. *J. Am. Chem. Soc.* **1991**, *113*, 706−7.
(32) Farr-Jones, S.; Basus, V. J. *Protein Society 7th Symposium* **1993**, poster 433T, San Diego.
(33) Basus, V. J.; Song, Q.; Hawrot, E. *Biochemistry* **1993**, *32*, 122.
(34) (a) St. Jacques, M.; Anet, F. A. L. *J. Am. Chem. Soc.* **1966**, *88*, 2585−6. (b) St. Jacques, M.; Anet, F. A. L. *J. Am. Chem. Soc.* **1966**, *88*, 2587−8. (c) Basus, V. J.; Anet, F. A. L. *J. Am. Chem. Soc.* **1973**, *95*, 4424−4426.
(35) Anet, F. A. L. *Fortschr. Chem. Forsch.* **1974**, *45*, 169.
(36) The "+" or " −" sign after the conformation name refers, respectively, to positive or negative helicity of the disulfide bond.

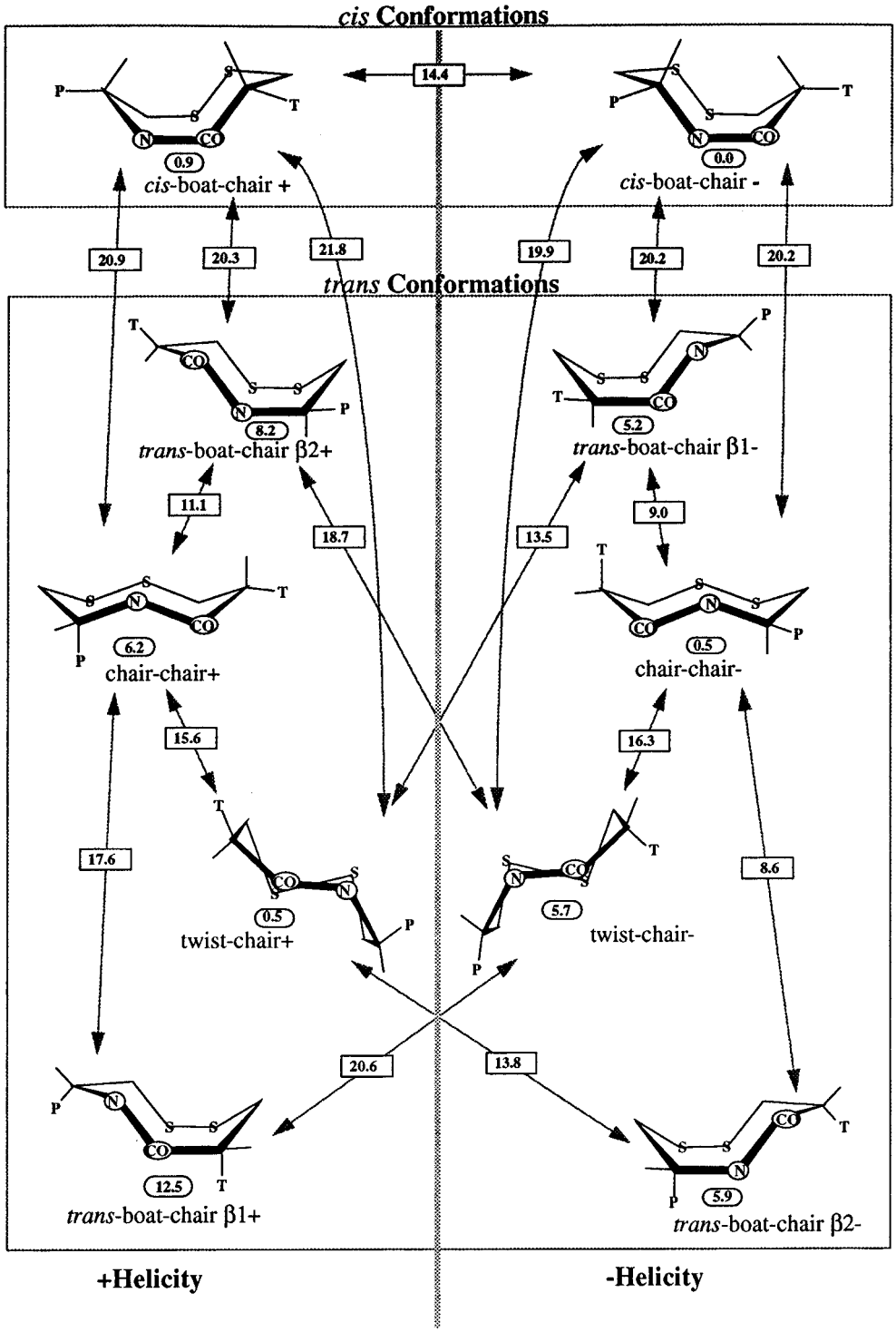

Figure 1. Predicted low energy conformations of TCCPD. Calculations were done with a modified molecule containing a methyl group in place of the residues PD and a methyl group in place of the threonine. Numbers below each structure are the calculated molecular mechanics energies relative to the lowest energy form (*cis*-boat-chair−). Barriers to interconversion between different conformations are indicated in rectangular boxes and are reported relative to the lowest energy conformation. All conformations in the left hand of the diagram have positive helicity for the disulfide bond, and those on the right have negative helicity.

the two *trans* conformations are expected to be rapidly interconverting in the NMR time scale.

Assignments and Conformational Characterization. Due to fast amide proton exchange, resonance assignments of TCCPD were carried out at pH 2.2, and −15 °C, in 30% methanol-d_3/70% water, using 11-echo water suppression techniques.[37] The one-dimensional spectrum collected at −15 °C shows a large number of amide resonances, indicating conformational heterogeneity since only three amide protons are expected in a rigid structure or in a set of rapidly interconverting structures. Using standard techniques,[38] four distinct TCCPD conformations were assigned (Table 1). The major (*A*) conformation and a minor (*B*) conformation had strong NOEs between the α-protons of C192 and C193 indicating very short distances (Figure 2a) only possible if both *A* and *B* have a *cis* amide bond between C192 and C193 (see Figure 1). These

(37) Sklenar, V.; Bax, A. *J. Magn. Reson.* **1987**, *74*, 469.

(38) Wuthrich, K. *NMR of Proteins and Nucleic Acids*; Wiley & Sons Inc.: New York, 1986.

Table 1. Chemical Shift Assignments for TCCPD at pH 2.2

T191	conformation	NH[a]	H_α[b]	C_α[c]	H_β[d]	C_β	H_γ	C_γ	H_δ	C_δ
44%	A (192-cis-193)	8.37	4.13	69.13	3.89	61.49	1.30	21.7		
18%	B (192-cis-193)		4.07	69.19	3.89	61.50	1.29	21.7		
23%	C (192-trans-193)		4.47	68.73	4.10	60.50	1.29	21.7		
15%	G		4.13	69.13	3.54	61.50	1.30	21.7		
C192										
	A (192-cis-193)	9.16	5.02	56.07	3.18	43.78				
	B (192-cis-193)	9.43	5.39	52.79	2.82	41.31				
	C (192-trans-193)	9.38	4.33	56.68	3.72g/3.40g	49.81				
	G	8.91	4.58	56.16	3.04	44.44				
C193										
	A (192-cis-193)	8.19	5.20	54.71	2.75g/3.46t	44.11				
	B (192-cis-193)	7.93	5.26	60.77	3.02t/3.14g	44.12				
	C (192-trans-193)	7.94	5.20	57.48	3.27	49.03				
	G	8.24	4.68	54.58	2.72t/3.33g	43.94				
P194										
	A (192-cis-193)		4.50	63.68	2.39/2.20	32.33	2.06	27.54	3.77/3.90	50.92
	B (192-cis-93)		4.45	63.64	2.20	32.11	2.00	24.35	3.68	50.75
	C (192-trans-193)		4.41	63.92	2.23/2.01	32.32	2.03	27.42	3.51	50.69
	G		4.68	63.22	2.45/2.29	34.92	1.89	24.94	3.51/3.70	50.71
D195										
	A (192-cis-193)	8.77	4.74	52.58	2.96	38.74				
	B (192-cis-193)	9.03	4.89	53.05						
	C (192-trans-193)									
	G	8.75	4.89	53.05	2.99/3.02	37.67				

[a] Exchangeable proton chemical shifts assigned at −15 °C. [b] Nonexchangeable chemical shifts reported at 15 °C. [c] Carbon chemical shifts reported at 15 °C. [d] β protons *gauche* and *trans* to the α-proton are indicated by the letters g and t, respectively.

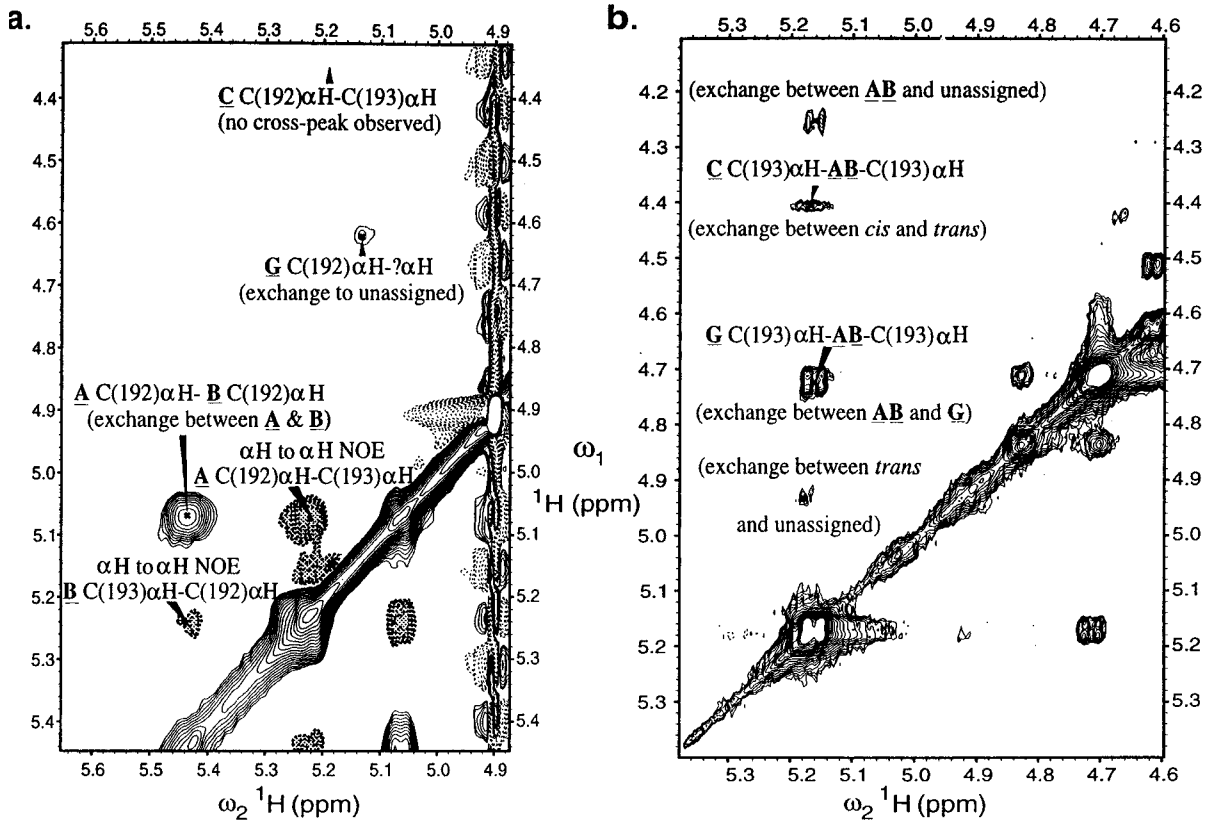

Figure 2. (a) A ROESY spectrum (75 ms mixing time) at 15 °C showing the exchange between the conformations *A* and *B* and exchange between conformation *G* and an unassigned conformation. This spectrum also shows the α-α-proton NOE cross-peaks proving that conformations *A* and *B* have a *cis* amide bond between C192 and C193. (b) A ROESY spectrum (75 ms mixing time) at 75 °C showing exchange between the *trans* conformation *C* and the coalesced *cis* conformations *AB*. Exchange is also observed between *G* and *AB* as well as *C* and other unassigned conformations.

two conformations differ only in the sign of disulfide bond dihedral angle. The least populated conformation, *G*, also has a *cis* amide bond between residues C192 and C193 based on the strong NOE observed between its α-protons. Since our calculations show that there are only two low energy *cis*-cysteinyl-cysteine rings, and we expect *cis-trans* isomerization about the proline bond, conformation G may have a *cis* amide bond between cysteine and proline residues, in addition to the *cis* cysteinyl-cysteine amide bond. However, due to spectral overlap, this could not be confirmed.

Conformation *C* shows no NOEs between α-protons indicating all *trans* amide bonds. From coupling constants and NOE cross-peak intensities, different *trans*-cysteinyl-cysteine conformations may be distinguished. Based on an NOE between

the amide protons of C192 and C193 and coupling constants of 7 Hz for both β-protons to α-proton of C192, the *trans* conformation in solution must have its amide protons in close proximity and have its C192 β-protons in a *gauche*−*gauche* orientation with respect to the α-proton. Unfortunately the β-proton resonances of C193 are degenerate. From this experimental information the *trans* conformation corresponds to either a twist-chair+ conformation or a chair-chair− conformation (see Figure 1). Our molecular mechanics calculations indicate a barrier of 13.0 kcal/mol between these two conformations. At room temperature, only a single set of peaks is observed, indicating a single conformation; however, at −15 °C exchange peaks are observed to an unidentified conformation whose population was too low for structural identification or kinetic analysis. Other conformations exist at various temperatures in solution, but their concentrations were not large enough to allow unambiguous assignments.

Observed Exchange Properties of TCCPD. To identify which conformations exchange, we collected ROESY spectra. ROESY experiments produce cross-peaks of opposite sign depending on whether the cross-peak results from conformational exchange or polarization transfer between protons (NOE). At low temperatures, −15 °C to 35 °C, conformations *A* and *B* exchange, as does conformation *G* and an unassigned conformer (Figure 2a). The exchange process at these low temperatures is most likely due to reorientation of the disulfide bond. By 35 °C the resonances of conformations *A* and *B* coalesce. The proton ROESY spectrum (Figure 2b) collected at 75 °C shows exchange between the *AB-cis* conformations (coalesced *A* and *B* conformations) and the *G* conformation, consistent with a high activation barrier between *cis* and *trans* proline conformations.[39] Figure 3b also shows exchange between the *AB-cis* conformations and the *C-trans* conformation, most likely due to rotation about the cysteinyl-cysteine amide bond. There are also exchange peaks between the *C-trans* conformations and other unassigned resonances. These peaks are generally weak, only exist at a few temperatures, and could not be assigned. The unassigned peaks are most likely due to the formation of other *trans*-cysteinyl-cysteine conformations or *cis*−*trans* proline isomerization. Furthermore, the α-protons of *AB* and *C* are strongly overlapping making exchange measurements with homonuclear-proton spectra impractical.

Since interconversion between the two *cis* conformations and between the *cis* and *trans* conformations is slow, it is possible to measure their exchange rates by NMR. Due to severe overlap of the proton spectra and to very efficient NOE-relayed exchange through the α-protons of the *cis* conformations, standard ^{1}H-exchange spectroscopy could not be used. Therefore, a modified HSQC pulse sequence[38−43] was used to measure conformational exchange via magnetization transfer to the carbon nucleus. This experiment gives well resolved proton-carbon correlation cross-peaks as well as exchange cross-peaks which are easily quantified (Figure 3). The data from the exchange experiments were used to solve the z-Bloch equations, giving the rate constants. Rate constants between 0.01 and 100 s^{-1} can be measured by this and similar techniques.[44] These rate constants are derived from a linear-weighted least-squares fit, as described by Perrin and co-workers.[44,45] The data weighting is dependent on the mixing time, with short mixing times weighted more heavily. Since each exchange-HSQC experiment takes approximately 18−24 h only a limited number of data points were collected. Approximately six points are necessary for an accurate exponential curve-fit, thus the linear weighted least squares-fit procedure is appropriate for this kind of data analysis.

Measurements made in the low temperature range (10 °C to 20 °C) yielded exchange rates between *cis*-cysteinyl-cysteine conformations *A* and *B*. The temperature range is narrow due to shifting of the residual water resonance down-field with decreasing temperature. At temperatures below 10 °C the residual water resonance overlaps the *A*-C192 α-carbon to α-proton cross-peak as well as the exchange peak from the *B*-C192 α-carbon. At temperatures greater than 20 °C, resonances of conformation *B* significantly broaden, making integration of HSQC peaks and the weaker exchange-peaks impossible. Figure 3 shows sample data collected at 15 °C. Integration of standard HSQC cross-peaks (Figure 3a) yields relative populations and, therefore, equilibrium constants. With a mixing time added to the pulse sequence, these cross-peaks as well as exchange cross-peaks could be integrated. The exchange-peaks for the lower temperature range ($A \rightarrow B$ and $B \rightarrow A$) were of equivalent intensity within signal-to-noise. A range of mixing times were collected to form exchange build-up curves. Only mixing times with linear exchange build-up were used, since other processes are significant at longer mixing times, as observed by the downward curvature of exchange-peak amplitude *vs.* mixing time plots. Figure 4 shows linear plots for conformation *A* converting to conformation *B* at three temperatures. The vertical bars on each data point are inversely proportional to the weight of the data point. At longer mixing times the vertical bars are larger due to lighter weighting. The exchange rates between conformations *A* and *B* are summarized in Table 2. Exchange between conformation *G* and *A* was not observed due to overlap in the carbon frequency. No other exchange processes were observed in this temperature range. Eyring plots were used to determine $\Delta H^{\ddagger}$ and approximate $\Delta S^{\ddagger}$ values. Associated errors in the activation energies were derived from Eyring plots of the rate constant plus and minus their standard deviations. This gives an envelope for the $\Delta H^{\ddagger}$ and $\Delta S^{\ddagger}$ values. The energetics calculated from Van't Hoff plots and Eyring plots are summarized in Table 3. The narrow temperature range in which exchange rates could be measured limits the accuracy of the activation entropy.

Exchange between *cis* and *trans* conformations proved to be more problematic than the low temperature exchange measurements discussed above. The final results are limited due to the small temperature range in which we were able to measure exchange (70−80 °C). At temperatures lower than 70 °C exchange is too slow to be measured by this technique. At temperatures above 80 °C, evaporation problems become serious even though the sample tube had a glass plug on top of the solution. Furthermore, the water resonance moved up-field, interfering with the observation of the resonances of interest. The α-protons used in the measurement of exchange between the two *cis* conformations are degenerate in the proton dimension and severely broadened at temperatures greater than 50 °C. The β-proton and β-carbon of the threonines from the *cis* conformations (*AB* and *G*) are totally overlapped yet remain well resolved from those of the *trans* conformation (*C*).

(39) (a) Wieland, T.; Birr, C. *International Review of Science, Org. Chem. Ser. 2*; Butterworth: London, 1976; v.6, pp 183−218. (b) Karle, I. L.; Karle, J.; Wieland, T.; Burgermeister, W.; Faulstich, H.; Wiktop, B. *Proc. Natl. Acad. Sci. U.S.A.* **1973**, *70*, 1836−1840.

(40) Wider, G.; Neri, D.; Wuthrich, K. *J. Biomol. NMR* **1991**, *1*, 93.

(41) Farrow, N. A.; Zhang, O.; Forman-Kay, J. K.; Kay, L. E. *J. Biomol. NMR* **1994**, *4*, 727−734.

(42) Montelione, G. T.; Wagner, G. *J. Am. Chem. Soc.* **1989**, *111*, 3096−3098.

(43) Johnston, E. R.; Dellwo, M. J.; Hendrix, J. *J. Magn. Reson.* **1986**, *66*, 399.

(44) Perrin, C. L.; Dweyer, T. J. *Chem. Rev.* **1990**, *90*, 935.

(45) Perrin, C. L.; Engler, R. *J. Magn. Reson.* **1990**, *90*, 363.

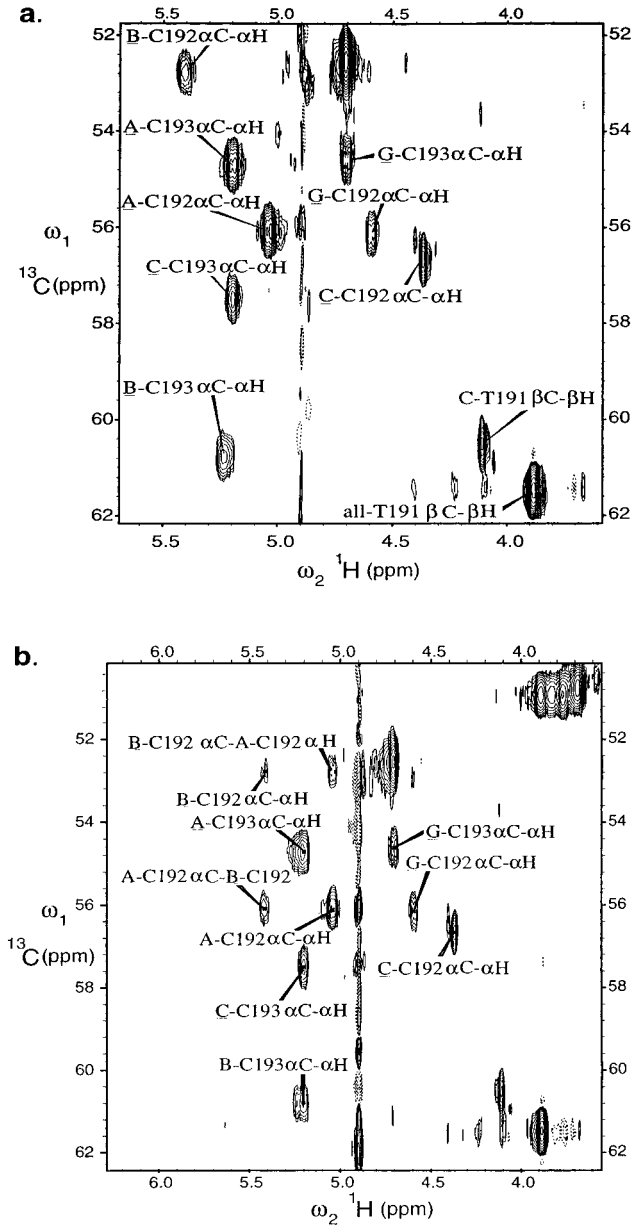

Figure 3. (a) The α-proton to α-carbon region of a standard HSQC showing the high resolution between the different conformations at 15 °C. (b) An HSQC-exchange experiment at 15 °C with a mixing time of 50 ms. Exchange peaks between conformation *A* and *B* are observed.

Exchange between *AB* and *G* could not be measured since no well resolved peaks were found in the high-temperature HSQC spectra. Figure 5 shows a standard HSQC spectrum (a) and an exchange-HSQC spectrum with a mixing time of 125 ms at 75 °C (b). At very short mixing times the exchange peaks were too weak to quantitate, while at longer mixing times (>200 ms) the exchange cross-peak intensity suffered losses from other relaxation processes. Exchange rates were measured at 70, 75 and 80 °C, summarized in Table 2. An Eyring plot was calculated in the same way as for the low temperature data. The energetics from the high temperature data are summarized in Table 3. These data should only be considered a rough estimate of the actual activation energies due to the lack of resolution between conformations *AB* and *C* as well as the limitations of the data discussed above. Comparisons of the ratio of exchange rate constants (rate forward over rate back) to the equilibrium constants are all within 10% for both high and low temperature data.

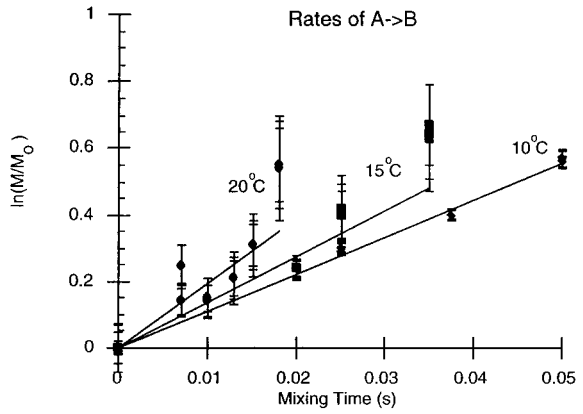

Figure 4. A plot of the matrix element *vs.* time for conformation *A* forming conformation *B* at three different temperatures. Vertical bars indicate the weighting of the data point in the weighted least-squares fit protocol.

Table 2. Rate Constants for Interconversion between *cis*-Cysteinyl-Cysteine Conformations, and between *cis*- and *trans*-Cysteinyl-Cysteine Conformations

temp (°C)	A → B (s^{-1}) major *cis*-CC to minor *cis*-CC	B → A (s^{-1}) minor *cis*-CC to major *cis*-CC
10	11.1 ± 0.2	26.7 ± 0.6
15	14 ± 1	34 ± 3
20	20 ± 2	50 ± 4
temp (°C)	**ABG → C (s^{-1}) *cis*-CC to *trans*-CC**	**C → ABG (s^{-1}) *cis*-CC to *trans*-CC**
70	0.20 ± 0.09	1.3 ± 0.8
75	0.31 ± 0.04	1.9 ± 0.2
80	0.55 ± 0.06	2.8 ± 0.6

Table 3. Experimentally Measured Energetics of TCCPD[b]

process	$\Delta G^{\ddagger}$ at 20 °C (kcal/mol)	ΔG at 20 °C[a] (kcal/mol)	$\Delta H^{\ddagger}$ (kcal/mol)	$\Delta S^{\ddagger}$ (cal/mol K)
cis(AB) → *trans*	21 ± 2	1.2 ± 0.2	24 ± 1	7 ± 3
trans → *cis*(AB)	21 ± 3		22 ± 2	5 ± 4
A → B	15 ± 4	0.48 ± 0.05	9 ± 2	−23 ± 6
B → A	15 ± 2		10 ± 1	−17 ± 4
A → C		0.34 ± 0.09		
A → G		1.0 ± 0.04		
C → B		0.10 ± 0.07		
B → G		0.53 ± 0.01		
C → G		0.7 ± 0.1		

[a] Measured from HSQC peak (no mixing time) intensities at 20 °C. [b] cis(AB) → *trans* and *trans* → cis(AB) energetics were calculated using the data collected at high temperatures, 70−80 °C.

Conclusions and Discussion

We showed that the pentapeptide fragment of AChR, TCCPD, can adopt at least four conformations in slow exchange on the NMR time scale. Two of these conformations have a *cis* peptide bond between the two cysteines forming an eight-membered ring. One conformation appears to have both a *cis* peptide bond between the cysteines and a *cis* peptide bond between cysteine-193 and proline-194 (conformation *G*). The fourth conformation has all *trans* peptide bonds. Exchange rates were measured between *cis* conformations *A* and *B* as well as between *cis* (*ABG*) and *trans* conformations (*C*). Exchange rates between conformation *G* and other conformations could not be measured due to overlap of both ^{1}H and ^{13}C chemical shifts.

It is interesting to compare the energetics of the TCCPD system to those calculated theoretically and to the energetics of the intact AChR. Values of ΔH, $\Delta H^{\ddagger}$, ΔS, and $\Delta S^{\ddagger}$ are difficult to determine accurately due to the small temperature

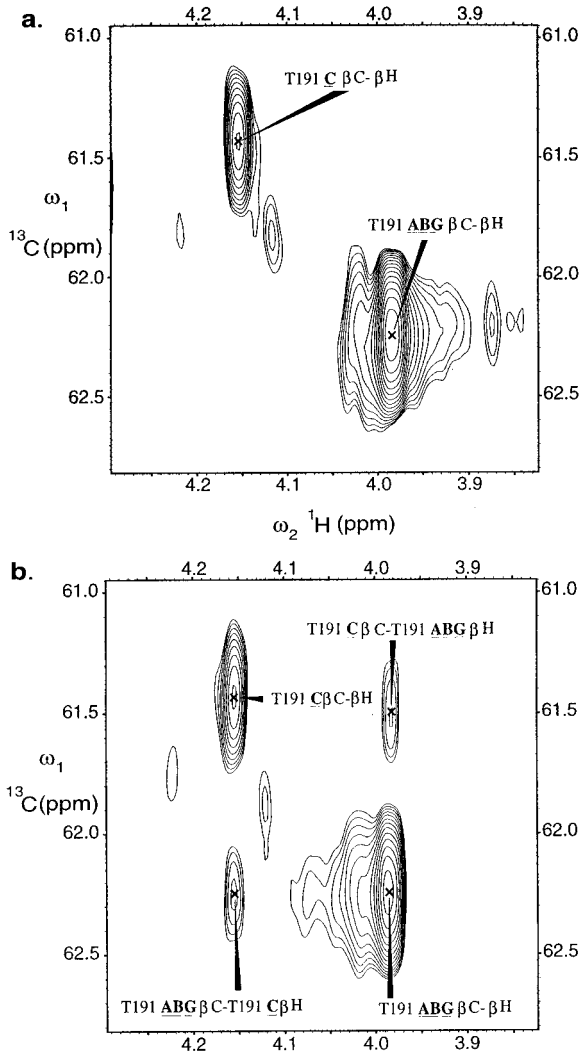

Figure 5. (a) HSQC and (b) exchange-HSQC with a mixing time of 125 ms at 75 °C showing the β-carbon and β-proton region of the threonine amino acid. The major peak corresponds to overlapped resonances of the *cis* conformations *A*, *B* and *G* while the minor resonance corresponds to the *trans* conformation *C*.

range for which exchange rates could be measured. Entropy differences between the different ring conformations are generally expected to be very small,[35] and we can assume that this is probably true for TCCPD. Thus we will compare the energy differences calculated by molecular mechanics between the different conformations directly with the ΔG and $\Delta G^{\ddagger}$ determined experimentally. Examining the energy barriers obtained by torsional driving, as shown in Figure 1, it is clear that the lowest energy conformation is the *cis*-boat-chair− conformation. From that conformation the lowest energy barrier is in converting to the *cis*-boat-chair+ conformation. The experimental ΔG between the two *cis* forms was 0.5 ± 0.1 kcal/mol, while the theoretical energy difference was 0.9 kcal/mol, and $\Delta G^{\ddagger} = 15 \pm 4$ kcal/mol, which is within experimental error of the calculated energy difference of 14.4 kcal/mol between the *cis*-boat-chair+ and the lowest energy transition state leading to the *cis*-boat-chair− conformation. Considering all paths leading from the *cis* conformations to the *trans* conformations, we find the lowest barrier to be 19.9 kcal/mol, while the experimental free energy of activation was 21 ± 2 kcal/mol, again within the experimental error. Only one trans conformation (*C*) was observed with $\Delta G_{AC} = 0.3 \pm 0.1$ kcal/mol. Molecular mechanics calculations (Figure 1) revealed several low energy conformations containing a trans amide bond between the two cysteines. Two were of low energy, within 1 kcal/mol of the lowest cis conformation. All other conformations had energies at least 5 kcal/mol higher and, therefore, are not expected to be significantly populated at the temperatures of our experimental measurements. Since our model in the calculations is somewhat different from the actual peptide used, it is possible that the energies calculated are slightly different from the experimental values (a 0.5 kcal/mol error is not unreasonable). It may be that the second *trans* conformation is actually of higher energy in the pentapeptide and is not significantly populated rather than simply in fast exchange. All experimental results, however, are consistent with either interpretation and with either of the two lowest energy *trans*-conformations being the major *trans*-conformation.

The activation barriers between the different states of the unliganded AChR may be quite high based on the very slow rates of spontaneous opening (1 to 7 s^{-1}).[13] Rates of spontaneous desensitization, to our knowledge, have not been measured directly but have been estimated to be about 0.2 s^{-1}.[46] The addition of acetylcholine to this system lowers these barriers allowing for channel opening or desensitization. Given that the barriers between the different states of the receptor are large and that the presence of the cysteinyl-cysteine ring is essential to proper receptor function, it seems quite plausible that changes in the structure of the disulfide ring may contribute significantly to the height of the receptor's activational barriers. Detailed structural analysis of the important conformations of the cysteinyl-cysteine ring shows that the two *cis* conformations are almost identical except for the position of the sulfur atoms, while the distance between the α-carbon atoms is longer by about 0.7 Å in the *trans* conformations compared to the *cis* conformations. Thus, while differences between the *cis* conformations are very subtle, the *cis* to *trans* interconversion could have significant consequences in the position of main chain atoms in a protein where the ring may function as a switch.

The occurrence of adjacent disulfide bonds is very rare suggesting an important biological role. In mercuric ion reductase the disulfide ring is believed to be important in binding the mercuric ion.[47] Vicinal disulfides are also conserved in the four known methanol dehydrogenases. The crystal structures show a trans disulfide ring with the conformation very similar to the chair-chair− in Figure 1, in close proximity to the pyrroloquinoline quinone (PPQ) . The ring may function as a molecular switch activating the enzyme: it could help secure or protect the PPQ, or it may function in a redox manner.[48]

The function of the strained ring formed by two adjacent cysteines is still open to speculation. Raman studies on the intact acetylcholine receptor in addition to structural studies of the extracellular portions of the α-subunit may help define the role of the cysteinyl-cysteine ring. The results presented here, on a peptide derived from the active site of the α-subunit of AChR, show that a cysteinyl-cysteine ring may form multiple stable conformations that may interconvert by overcoming high activation barriers in solution. Although a peptide cannot model the complexity of a protein, it is possible that structural changes in the cysteinyl-cysteine ring may act as a molecular switch in the context of a protein.

(46) Franke, Ch.; Parnas, H.; Hovav, G.; Dudel, J. *Biophys. J.* **1993**, *64*, 339−356.
(47) Schierling, N.; Kabasch, W.; Moore, M. J.; Distefano, M. D.; Walsh, C. T.; Pai, E. F. *Nature* **1991**, *354*, 168−172.
(48) (a) White, S.; Boyde, G.; Mathews, F. S.; Xia, Z.-X.; Dain, W.-W.; Zhang, Y.-F.; Davidson, V. L. *Biochemistry* **1993**, *32*, 12955−12958. (b) Chosh, M.; Anthony, C.; Harlosk, Goodwin, M. G.; Blake, C. *Structure* **1995**, *3*, 177−187.

Experimental Methods

Molecular Modeling. All calculations were carried out using AMBER v4.1 with the Cornell *et al*.[49] force field. We used the interface to AMBER[50] to control the AMBER calculations. Initial molecular models were built manually using LEaP, a module of the AMBER suite of programs.[51] Models were built with a methyl replacing the NH atoms of C192 together with the previous threonine and a methyl replacing the carbonyl of C193 together with the following proline and aspartic acid residues. Refinement of the initial model structures was done using energy minimization carried out *in vacuo*, without a non-bonded cut-off. Minimization was carried out with 100 steps of steepest descent minimization followed by conjugate gradient minimization for the remainder to an rms energy deviation of 1×10^{-5} kcal/mol.

The activation barriers to interconversion between ring forms were determined using torsional driving. Energy minimization of the model peptide was carried out in two degree increments of the driven torsional angle. The force constant for the constraint was 400 kcal mol^{-1} $radian^{-2}$. This rather large force constant was required to overcome the strain in the eight-membered ring. This protocol was repeated in both directions, i.e. converting one ring conformation to another and back.

Synthesis. The pentapeptide, T(OtBu)-C(acm)-C(acm)-P-D(OtBu)-PAC support, was synthesized automatically on an Applied Biosystems 431A peptide synthesizer using solid state Fmoc chemistry.[52] F-moc amino acids were purchased from Millipore Corporation (Bedford MA). The resin-bound peptide was oxidized by a modified procedure of Albericio *et al*.[53] A 100 mg sample of the peptide-resin was suspended in 7 mL of 5% anisole and 95% N-methylpyrrolidine (NMP) at room temperature. Ten equivalents of iodine (~94 mg) were dissolved in 3 mL of the anisole/NMP solvent. The iodine solution was added to the resin suspension over a period of ten minutes. The mixture was allowed to react for 10 h with stirring, and then the resin was collected on a medium sintered glass filter and washed six times with 3 mL of anisol/NMP and six times with 3 mL of absolute ethanol. The oxidized peptide was then cleaved and deprotected in 95% trifluoroacetic acid and 5% water. The resin was removed by filtration, and the filtrate was concentrated and cooled. The peptide was recovered by cold ether precipitation and purified by FPLC using a reverse phase preparatory column (Pep RPC 16/10, Pharmacia Inc.). Three peaks eluted with a water/acetonitrile (0.1% TFA) 0−20% gradient over 40 min. Electrospray mass spectroscopy confirmed that the first peak eluted was a monomer of 536.2 mu, while the second and third peaks were dimers.

NMR. For the ^{1}H-NMR spectra, 25 ± 3 mM peptide was dissolved in water (10% D_2O/90% H_2O). For the heteronuclear experiments the peptide was dissolved in D_2O for a final concentration of 60 ± 5 mM. Sample concentrations were determined by comparing the methyl NMR peak intensity to that of the internal standard (TSP) peak intensity with known concentration. The pH value for all samples was 2.2 ± 0.2.

(a) Homonuclear Experiments. NMR data were collected on either a GN500, Omega500 or a Unity Plus 600 MHz spectrometer. The data were processed using STRIKER and SPARKY programs.[54,55] Assignments were made at −15 °C in 60% H_2O, 30% methanol-d_3, and 10% D_2O. In order not to suppress the amide proton resonances SNOESY[56] or 11-echo-NOESY[37] spectra were collected at 600 MHz or 500 MHz with a mixing time of 150 ms. Mixing times for NOESY spectra collected in H_2O at temperatures from −15 to 15 °C ranged from 75 ms to 200 ms. To identify which cross-peaks were due to conformational exchange, ROESY spectra were collected in water with 11-echo water suppression[57] and a mixing time of 75 ms. ROESY spectra were also collected in D_2O with a 75 ms mixing time at temperatures ranging from −15 to 85 °C. TOCSY spectra were collected in water with a 11-echo[37] water sequence with a 70 ms mixing time at temperatures −15 to 15 °C. TOCSY spectra were also collected in D_2O with 70 ms mixing times over a temperature range of 10 to 85 °C. Exclusive COSY[58] spectra were collected at both 15 °C and 65 °C. All proton spectra were collected with 32 to 48 scans per block, and 400−512 points in t_1 (zero-filled to 1024 pts) and 4096 points in t_2. All data, except for ECOSY and ROESY spectra, were apodized with a sinebell squared function phase shifted 80° (phase shifted 55° for ECOSY spectra).

(b) Heteronuclear Experiments. HSQC[59] and HSQC-TOCSY[60] experiments were used to assign ^{13}C resonances. To measure the exchange rates between conformations an HSQC pulse sequence was modified in a way very similar to that of Montelione & Wagner.[42] A BIRD[61] sequence was used to suppress ^{1}H(-^{12}C) resonances followed by an INEPT[62] transfer of magnetization to the ^{13}C-nuclei whose chemical shift was allowed to evolve during t_1 (with proton refocussing). During the t_1-evolution time, the carbon magnetization is in the *xy*-plane. It is then flipped by a 90° pulse onto the -*z*-axis where exchange between the different conformations occurs during the mixing period (exchange between I_zS_z spin-states). Following the mixing period, the magnetization is transferred back to the protons via the reverse-INEPT sequence and data is acquired with Garp[63] carbon decoupling.

Exchange-HSQC spectra where collected with 1720 points in t_2 and 72 (high temperature data) to 96 (low temperature data) points in t_1 on the 600 MHz spectrometer. The delay between each acquisition was 3 s for the low temperature data and 4 s for the high temperature data. The sweep width in ω_1 was 9000 Hz centered at 41 ppm for the low temperature range, and 3922 Hz centered at 64 ppm for the high temperature range. The sweep width in ω_2 was 6500 Hz centered on water for both high and low temperature data acquisition. Data was apodized with a sine squared function phase shifted 90° in both dimensions. Cross-peaks were integrated using a surface Gaussian fit routine within SPARKY.

Calculation of Exchange Rates. Traditionally, 2D exchange experiments involve analysis of cross-peak amplitudes with multi-exponential data fitting if more than two species exchange. Since it could have been the case here that we would have more than two pentapeptide isomers involved in exchange at higher temperatures, we used data analysis techniques established by Prof. Charles Perrin.[44,45] The advantage of this technique is that it employs a relaxation matrix method to calculate exchange rates. Each off-diagonal element connects one species to another allowing for exponential fit of all data simultaneously. In addition, data fitting routines were improved by using a weighted least-squares approach. Since data collected at longer mixing times are less accurate, their importance in the final solution is down-weighted.[35] The process is described by solving the *z*-Bloch equations

$$\mathbf{A} = \exp(-\mathbf{R}t_m) \tag{1}$$

where matrices **A** and **R** are given by

(49) Cornell, W. D.; Cieplak, P.; Bayly, C. I.; Gould, I. R.; Merz, K. M.; Ferguson, D. M.; Spellmeyer, D. C.; Fox, T.; Caldwell, J. W.; Kollman, P. A. *J. Am. Chem. Soc.* **1995**, *117*, 5179−5197.

(50) Pearlman, D. A. *Amber/Interface*; Copyright David A. Pearlman, 1993.

(51) Pearlman, D. A.; Case, D. A.; Caldwell, J. W.; Ross, W. S.; Cheatham, T. E.; Ferguson, D. M.; Seibel, G. L.; Singh, U. C.; Weiner, P. K.; Kollman, P. A. *Amber 4.1*; Copyright U. C. Regents, 1995.

(52) Barany, G.; Merrifield, R. B. In *The Peptides*; Gross, E., Meienhofer, J., Eds.; Academic Press: New York, NY, 1980; Vol. 2.

(53) Albericio, F.; Hammer, R. P.; Carcia-Echeverria, C.; Molins, M. A.; Chang, J. L.; Munson, M. C.; Pons, M.; Giralt, E.; Barany, G. *Int. J. Pept. Protein Res.* **1991**, *37*, 402.

(54) Day, M.; Kuntz, I. D. *Striker*; Copyright, U. C. Regents, 1993.

(55) Kneller, D.; Kuntz, I. D. *Sparky*; Copyright, U. C. Regents, 1993.

(56) Smallcomb, S. *J. Am. Chem. Soc.* **1993**, *115*, 4776.

(57) Bax, A. *J. Am. Chem. Soc.* **1987**, *109*, 6511−6513.

(58) Griesinger, C.; Sørensen, O. W.; Ernst, R. R. *J. Am. Chem. Soc.* **1985**, *107*, 6394.

(59) Bodenhausen, G.; Ruben, D. J. *Chem. Phys. Lett.* **1980**, *69*, 185.

(60) Lerner, L.; Bax, A. *J. Magn. Reson.* **1986**, *69*, 375.

(61) Garbow, J. R.; Weitekamp, D. P.; Pines, A. *Chem. Phys. Lett.* **1982**, *93*, 504.

(62) Morris, G. A.; Freeman, R. *J. Am. Chem. Soc.* **1979**, *101*, 760.

(63) Shaka, A. J.; Barker, P. B.; Freeman, R. *J. Magn. Reson.* **1985**, *64*, 547.

$$\mathrm{A} = \begin{matrix} \frac{a(t_m)AA}{A_o} & \frac{a(t_m)AB}{B_o} & \frac{a(t_m)AC}{C_o} \\ \frac{a(t_m)BA}{A_o} & \frac{a(t_m)BB}{B_o} & \frac{a(t_m)BC}{C_o} \quad \frac{a(t_m)CC}{C_o} \\ \frac{a(t_m)CA}{A_o} & \frac{a(t_m)CB}{B_o} \end{matrix} \quad \mathrm{R} = \begin{bmatrix} -\rho_A & k_{BA} & k_{CA} \\ k_{AB} & -\rho_B & k_{CB} \\ k_{AC} & k_{BC} & -\rho_C \end{bmatrix} \tag{2}$$

R contains the dynamic parameters to be determined while **A** contains the measurable NMR quantities. In **A** the quantities $a(t_m)_{AA}$, $a(t_m)_{AB}$, ... are the 2D peak amplitudes measured in an exchange experiment, such as the HSQC-exchange experiment, with mixing time t_m and A_o, B_o, ..., the HSQC peak amplitudes measured at $t_m = 0.00$. The matrix **A** can be written in terms of its eigenvector decomposition as

$$\mathbf{A} = \mathbf{X}\,\Lambda\,\mathrm{X}^{-1} \tag{3}$$

where **X** is the matrix of column eigenvectors of **A** and Λ is the diagonal matrix of eigenvalues. The Bloch equation can be linearized by substituting (3) into (1) and taking the natural logarithm

$$\ln(\mathbf{A}) = \mathbf{X}(\ln\Lambda)\mathrm{X}^{-1} \tag{4}$$

A plot of the elements of $\ln(\mathbf{A})$ vs. t_m will give a straight line with a the slope of either ρ_A, ρ_B (the relaxation rate) or $-k_{AB}$, $-k_{BC}$, etc. (the rate constant). The straight line can then be fit with a weighted least-squares protocol. One advantage of this technique is that only three data points are necessary for a line fit, although approximately six points are necessary for a good exponential curve fit.

Acknowledgment. We thank Dr. P. A. Kollman for his assistance with the molecular mechanics calculations and Drs. E. Hawrot, L. N. Gentile, D. A. Pearlman and R. Cerpa for helpful discussions. Mass spectral analysis was provided by the UCSF Mass Spectrometry Facility supported by the Biomedical Research Technology Program of the National Center for Research Resources (NIH NCRR BRTP 01614). Molecular Graphics were done using the UCSF Computer Graphics Laboratory (NIH RR-1081). This work was supported by NSF, and the Committee on Research of the Academic Senate, UCSF.

JA962005V